ACS APPLIED MATERIALS & INTERFACES

Research Article

www.acsami.org

Viscous Conductive Glue Layer in Semitransparent Polymer-Based Solar Cells Fabricated by a Lamination Process

Chieko Shimada and Seimei Shiratori*

School of Integrated Design Engineering, Keio University, Minato, Tokyo 108-8345, Japan

ABSTRACT: Semitransparent polymer-based solar cells were fabricated by using a low-cost, vacuum-free lamination process. This process is to deposit a conductive glue solution on the transparent Ag film, followed by lamination with the active layer. The glue solution and a mixture of poly(3,4-ethylenedioxythiophene): poly(styrenesulfonate) (PEDOT:PSS) and D-sorbitol was used. To allow future improvements in the conversion efficiency of these cells, we investigated the relationship between major factors of the conductive glue layer and photovoltaic property. As a result, it was suggested that photovoltaic property had less of a relation to conductivity of the conductive glue layer but a strong correlation with the contact area within a certain range of the film thickness of the conductive glue layer. The optimized cells exhibited 2.22% and 2.41% of power conversion efficiencies during front and backside 100 mW cm^{-2} AM1.5G illumination with reflection paper, respectively.

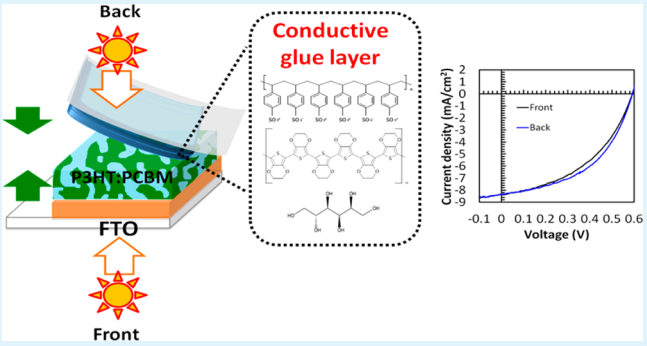

KEYWORDS: *solar cells, PEDOT:PSS, D-sorbitol, lamination, glue, contact area*

INTRODUCTION

Semitransparent solar cells are expected to have applications in the design of bifacial power generating windows. Especially, polymer-based bulk heterojunction solar cells have attracted significant attention partly because their improved optical transmittance makes them well suited to the fabrication of bifacial power generating windows.[1−6]

Polymer-based solar cells are fabricated at low cost because the active layer is prepared by simple solution processing. However, it is also standard practice to use vapor deposition, a vacuum process, to fabricate the thin metal electrodes of polymer-based cells especially in the case of semitransparent polymer-based cells. The use of these techniques results in relatively high fabrication costs, which is disadvantageous.

To date, several studies concerning the fabrication of semitransparent polymer-based solar cells using a wet process have been reported.[6−12] These approaches, however, suffer from rapid degradation in response to oxygen and moisture intrusion, since the hygroscopic conductive polymeric electrode is exposed to atmospheric air. In addition, it is a problem that conjugated polymers,[13,14] which are used as active materials, are highly sensitive to oxidation or moisture.[15−17] A total loss of efficiency by more than 60% within 2 h of exposure to dry synthetic air was reported.[18] Therefore, it is necessary to encapsulate the solar cell, preventing the exposure of the active materials to oxygen and water.

Recently, a hot press lamination process has been reported for the fabrication of metal electrode on the active layer of polymer-based solar cells.[19−21] A fabrication process based on lamination is expected to reduce the fabrication cost because the complex equipment is not required. Moreover, this method has the capacity to produce encapsulated devices that are resistant to mechanical stress and moisture intrusion. However, they do not discuss the details of the condition of the conductive interlayer and resistance to degradation of this lamination process. In addition, the conductive interlayer by the other lamination methods is easy to peel off because the glue solution without sorbitol did not have enough viscosity to attach and fix two electrodes. In this study, we used the lamination process, which was to deposit "a viscous conductive glue solution" on the Ag film, followed by lamination with the active layer. The efficiency of the bifacial solar cells may be lower than that using conventional Al electrode; however, they will open the possibility for the usage of the solar cells as the power windows that can be used by both daytime sunshine and artificial light at night which usually has incident light from the opposite direction of daytime. In addition, they may open the possibility of semitransparent wind or a sound barrier that may be used along the road or field.

A transparent Ag nanonetwork film, formed by the self-organization of a three-dimensional Ag network, was used as the metal electrode in our cells. Since this Ag nanonetwork incorporates unfilled regions of 100−200 μm in size, it may be employed to fabricate semitransparent solar cells capable of bifacial incident light absorption. The height of the nanonetwork is approximately 3 μm. As well, since the Ag electrode

Received: August 9, 2013
Accepted: October 18, 2013
Published: October 18, 2013

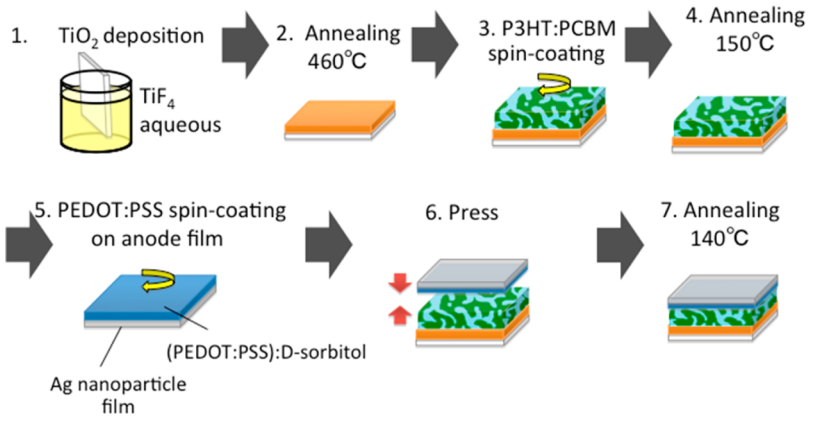

Figure 1. Solar cell fabrication process.

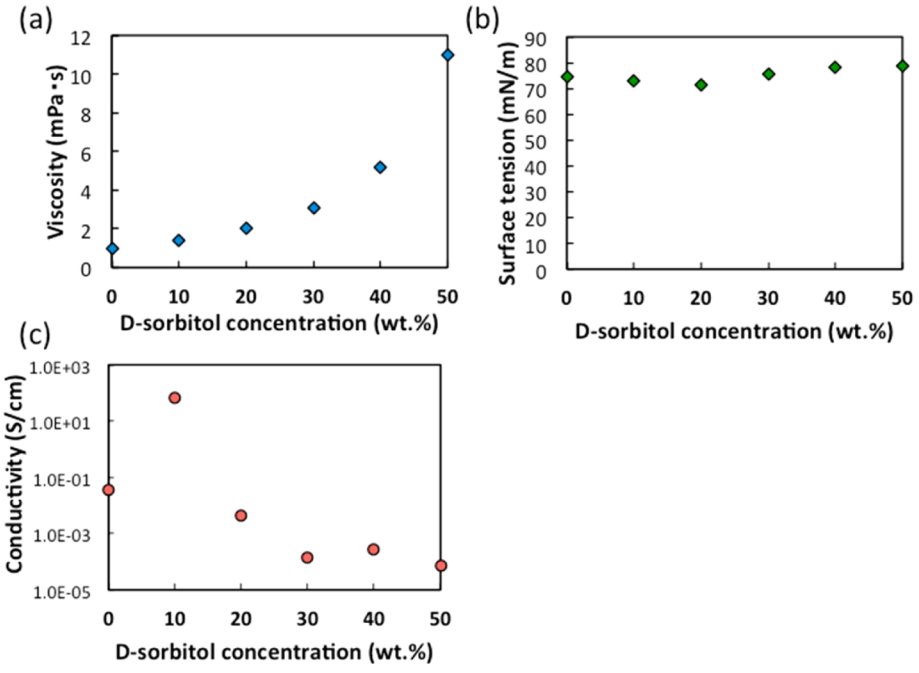

Figure 2. (a) Viscosity, (b) surface tension of the conductive glue solution, and (c) conductivity of glue layer coated on the glass substrate for different D-sorbitol concentrations.

material is highly transparent to visible light, incident light is absorbed primarily by the semiconductor and fullerene compounds contained in the polymer.

To enhance the energy conversion efficiency, the morphology of the active layer is an important factor. In this study, the conductive glue layer was the focus. It is crucial to understand the relationship between the factors of the glue layer and photovoltaic property. The goal of this study is to clarify the important factor related to photovoltaic property in the conductive glue layer for the device optimization and to verify the resistance to degradation. The major factors related to the photovoltaic property are considered to be work function, conductivity, film thickness, and contact area. In particular, it was reported that conductivity was important for carrier transport.[22] In this work, poly(3,4-ethylenedioxythiophene):poly(styrenesulfonate) (PEDOT:PSS) and D-sorbitol were used as a conductive glue layer and its additive, respectively. It is considered that the addition of D-sorbitol changes the physical properties of the conductive glue layer, such as work function, viscosity, surface tension, and conductivity. We considered that these physical property changes affected the photovoltaic property and investigated the effects on the photovoltaic property by adding D-sorbitol.

EXPERIMENTAL DETAILS

Figure 1 illustrates the steps involved in fabrication of experimental solar cells with the structure FTO/TiO_2/P3HT:PCBM/PEDOT:PSS/Ag-nanoparticles (NP). An initial TiO_2 layer was prepared by immersing a fluorine-doped tin oxide (FTO; 7 Ω/□, 80%, SPD Laboratory) glass slide in an aqueous TiF_4 solution (pH 2.0) at 60 °C inside a controlled temperature cabinet (Tabai LC-112), followed by annealing at 460 °C via a hot plate (Iwaki PC-35). The blend solutions of poly(3-hexylthiophene) (P3HT) and [6,6]-phenyl C61-butyric acid methylester (PCBM) were prepared at concentrations of 50 mg per mL of monochlorobenzene (Wako Chemical). The weight ratio of P3HT and PCBM was 1:1. These mixtures were spin-coated at 1200 rpm onto the TiO_2 layer and then annealed at 150 °C for 15 min using a hot plate. Simultaneously, the PEDOT:PSS solution (PH500, Clevious) with D-sorbitol (Wako Chemical) was spin-coated at 3000 rpm on a Ag NP film (Toda Kogyo Corp.). This Ag NP forms a

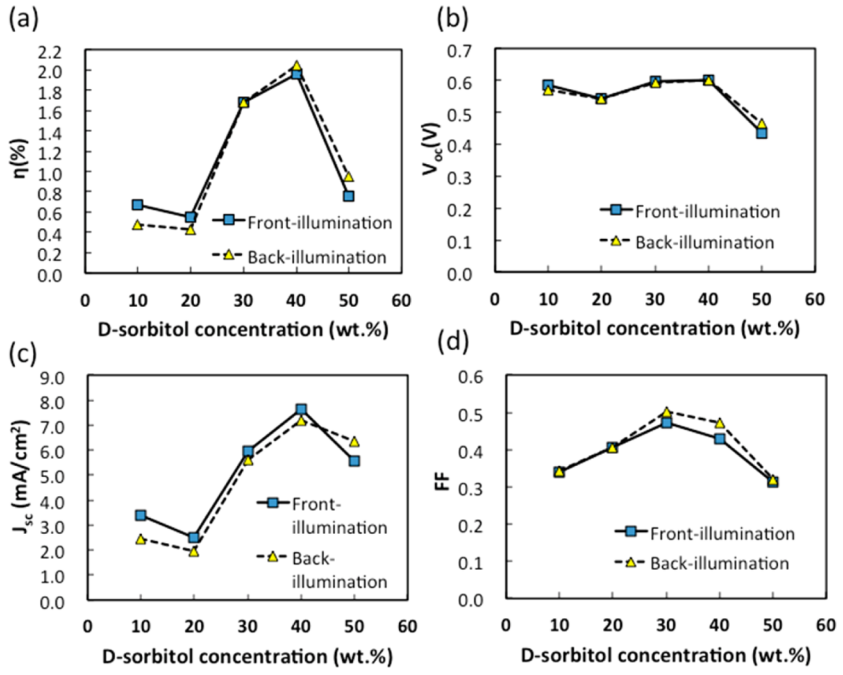

Figure 3. Variations in (a) energy conversion efficiency (η), (b) open-circuit voltage (V_{oc}), (c) short current density (J_{sc}), and (d) fill factor (FF) for samples with varying D-sorbitol concentrations.

conducting network, and its conductivity was 10 Ω/□ on PET film substrate, which was used as top electrode.[23] With the spin coating technique, the gaps between the Ag NP networks were infilled by the PEDOT:PSS and semitransparent conducting electrodes for the solar cells were fabricated. The thickness of the active layer was measured as 221 nm by using a Dektak 3030 profile meter. The active area of the devices are all 0.2827 cm^2. D-Sorbitol concentration was varied from 10% to 50%. Immediately afterwards, the finished solar cells were fabricated by pressing the active layer component and the Ag film component together at approximately 0.1 MPa. Then, the devices were annealed at 140 °C for 3 min.

The current density−voltage ($J-V$) characteristics of the solar cells were measured using an AM1.5 solar simulator (100 mW cm^{-2}) consisting of an optical power multimeter (Advantest TQ8215) and an automatic polarization system (Hokuto Denko HSV-100) with a 500 W Xe lamp (Ushio UXL-500SX). A mask was used to create an exposure area of 0.28 cm^2 for all samples. The light transmittance of each cell was measured via UV−vis spectroscopy (Shimadzu UVmini-1240). A tensile tester (Shimadzu, EZ-Test) was used to observe shear strength of the glue layer. The sheet conductivity was measured using a four points probe (Mitsubishi Chemical Analytech, MCP-T610). The cross-sectional images of the cells were observed by a digital microscope (Keyence, VHX-1000). Two devices were fabricated for each composition. We selected the first data for each point, and the second data were used to confirm the data were reproducible within 5% error.

RESULTS AND DISCUSSION

1. Physical Property Changes at Different D-Sorbitol Concentrations. Figure 2a,b shows plots of the viscosity and surface tension at different concentrations of D-sorbitol in PEDOT:PSS solution. The conductivity of PEDOT:PSS(D-sorbitol) film coated on glass was measured by the 4-point probe technique shown in Figure 2c. In Figure 2a, the viscosity exponentially increased with an increase in D-sorbitol, especially at more than 50% of D-sorbitol concentration. One D-sorbitol molecule has six hydroxyl groups. When the ratio of D-sorbitol increased, hydrogen bonds were formed among D-sorbitol molecules. This molecule interaction caused the higher viscosity of mixed solution of PEDOT:PSS and D-sorbitol. As shown in Figure 2b, the major change was not observed at surface tension. In Figure 2c, the conductivity increased by addition of 10 wt % of D-sorbitol ($3.46 \times 10^{-2} \rightarrow 6.86 \times 10^{-2}$ S/cm). At concentrations above 10 wt %, however, the conductivity decreased with increasing D-sorbitol concentration. At 50 wt %, the glue layer was almost in an insulating state. It was reported that, in addition to D-sorbitol into the PEDOT:PSS solution, its work function decreased and was saturated at approximately 4.85 eV at concentrations above 5 wt %.[24] Therefore, it was considered that there was a little change in work function in the addition range of 10−50 wt % in this work.

2. *J*−*V* Characterization. Figure 3a−d shows plots of the energy conversion efficiency (η), open-circuit voltage (V_{oc}), the short-circuit current density (J_{sc}), and fill factor (FF) at different concentrations of D-sorbitol in PH500 which were measured under a 100 mW/cm^2 AM1.5 solar simulator. Table 1 shows these values. In this experiment, the device containing no sorbitol did not show the photovoltaic characteristics. This is because the glue solution without sorbitol did not have enough viscosity to attach and fix two electrodes. The device in this condition was easily breakable. Though the detailed results are going to be published elsewhere, we considered that the performance of such cells during both front and backside illumination is affected by phase separation of the p- and n-type organic semiconductors.

Since the cells fabricated in this study had a high transmittance as shown in Figure 4a,b, the cells may generate energy from either front or backside illumination, and "Front-illumination" and "Back-illumination" in Figure 3 refer to irradiation of the device from the FTO side or Ag NP film side, respectively.

As shown in these figures, the best device performance is obtained using a D-sorbitol concentration of 40 wt %. In to 20−40 wt % range, η increased with increasing additive ratio. At

Table 1. Photovoltaic Characteristics for Samples with Varying D-Sorbitol Concentrations[a]

	D-sorbitol concentration	V_{oc} (V)	J_{sc} (mA/cm^2)	FF	η (%)
front-illumination	10 wt %	0.59	3.38	0.34	0.67
	20 wt %	0.54	2.50	0.40	0.55
	30 wt %	0.60	5.95	0.47	1.68
	40 wt %	0.60	7.64	0.43	1.96
	50 wt %	0.44	5.55	0.31	0.75
	40 wt % with RP	0.60	8.35	0.44	2.22
back-illumination	10 wt %	0.57	2.44	0.34	0.48
	20 wt %	0.54	1.95	0.41	0.43
	30 wt %	0.59	5.62	0.50	1.68
	40 wt %	0.60	7.20	0.47	2.05
	50 wt %	0.44	5.55	0.31	0.75
	40 wt % with RP	0.61	8.33	0.48	2.41

[a]RP refers to a reflection paper.

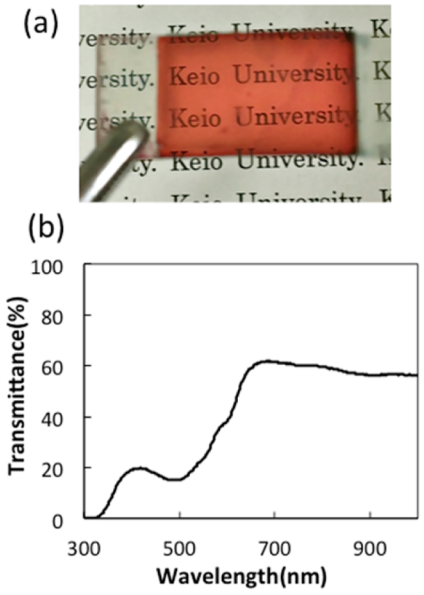

Figure 4. (a) Image and (b) transmittance of the device in this study.

concentrations above 40 wt %, however, η dramatically decreased. At concentrations below 20 wt %, the large difference of η was not observed. In Figure 3b, there was little change in V_{oc} in the 10−40 wt % range. At concentrations above 40 wt %, however, V_{oc} decreased. In Figure 3d, FF was steadily increasing at 10−30 wt % and then decreasing. Since the fabricated devices are semitransparent, the FF values are relatively low compared with the nontransparent solar cells using Al electrodes;[6] however, we believe that it will not affect the study of adding D-sorbitol in the adhesive layer. In Figure 3c, the behavior of J_{sc} was similar to that of η. From this figure, it was thought that J_{sc} had a considerable effect on photovoltaic property.

To utilize the high transmittance of the cells, the quantity of light absorption may increase by using reflection paper (RP) beneath the cell during AM1.5 illumination. By using RP, η went up by 13−18%, and η with back illumination was 2.41% as shown in Table 1. In addition, Figure 5 shows η normalized to the initial values for the sample. In the case when D-sorbitol was used, the optimized sample maintained the photovoltaic property for 3 weeks at room temperature. In this figure, to

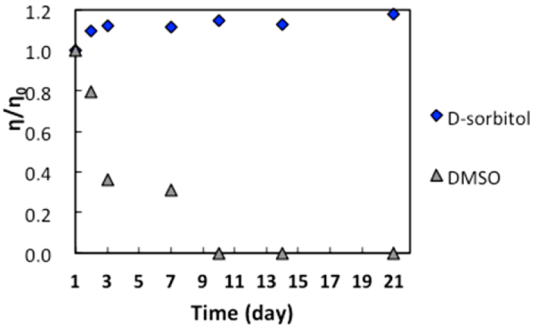

Figure 5. η normalized to the initial values for the optimized sample.

confirm the effect of D-sorbitol, DMSO was added at the same quantity, instead of D-sorbitol, and compared.

Interestingly, conductivity of glue solution was not an important factor for the photovoltaic property, from Figures 2c and 3a. We investigated the effects of the film thickness and contact area on the photovoltaic property.

2.1. Film Thickness. Figure 6a−c shows cross-sectional images of the thin films that mimicked the actual solar cells

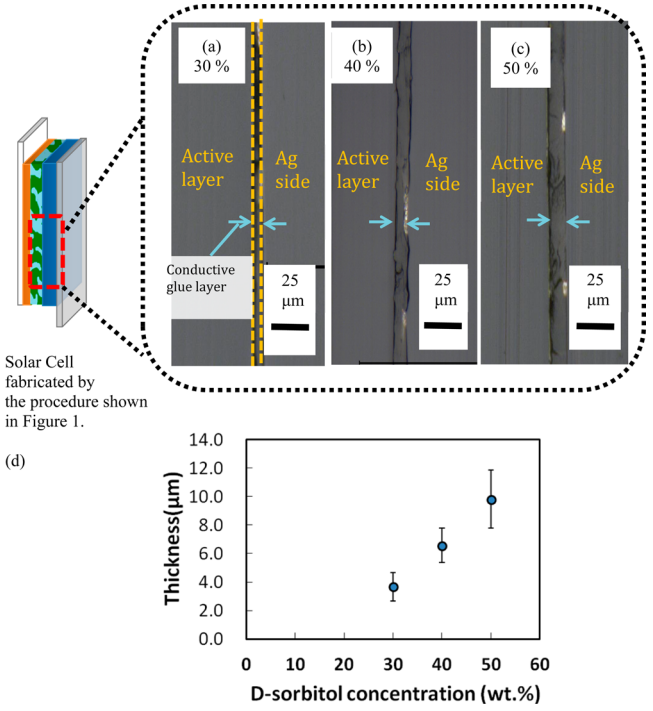

Figure 6. (a−c) Cross-sectional images at D-sorbitol concentrations of (a) 30 wt %, (b) 40 wt %, and (c) 50 wt % and (d) the relationship between D-sorbitol concentration and the film thickness of the glue layer. The structure of the cells were PET film/P3HT:PCBM/PH500(D-sorbitol)/Ag PET film.

obtained by the digital microscope. The structure of the cells were PET film/P3HT:PCBM/PH500(D-sorbitol)/Ag PET film. The right side of the images shows Ag nanonetwork film. The left side shows P3HT:PCBM surface on PET film. The gap between Ag film and the active layer is the glue layer. The white shining grains are the cross-sectional Ag nanonetwork. Because the film was fragile due to the 3.12 ± 0.76 μm-high Ag network, the film thickness whose concentration was less than 20 wt % was unmeasured. Figure 6d displays plots of the film thickness at different D-sorbitol concentrations of glue

dx.doi.org/10.1021/am402698x | ACS Appl. Mater. Interfaces 2013, 5, 11087−11092

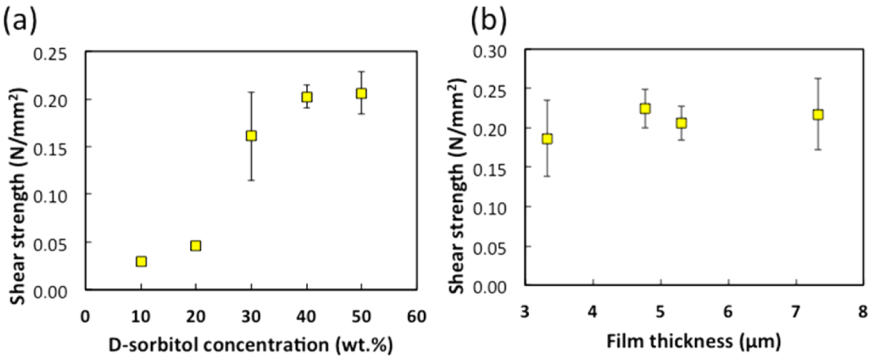

Figure 7. Shear stress of the conductive glue layer (a) with different D-sorbitol concentration and (b) with the fixed D-sorbitol concentration and different film thickness.

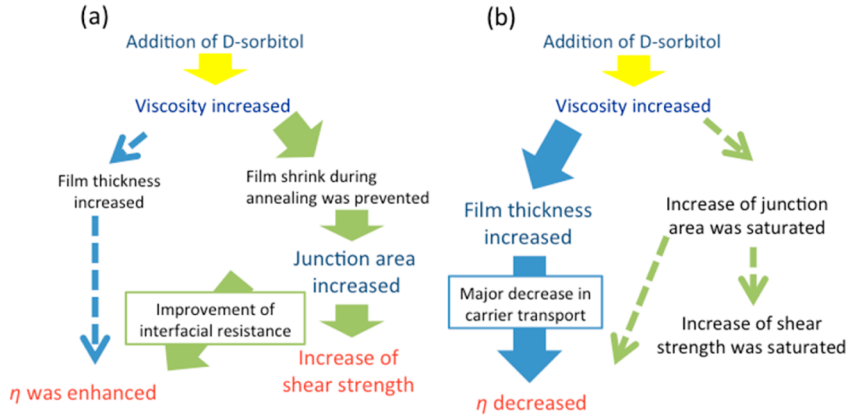

Figure 8. Flow charts of effects of the (a) low and (b) high concentrations of D-sorbitol on the efficiency.

solution from these images. In the cases of D-sorbitol concentration above 30 wt %, the film thickness increased as viscosity increased.

The PEDOT with D-sorbitol layer deposited on Ag nanonetwork film was annealed at 140 °C for 3 min. Since the melting point of D-sorbitol was 95°C, it is necessary for it to be melted to act as glue. By this annealing, the moisture in the device may not fully be removed; however, all the devices are treated in the same way because we found that long annealing resulted in decrease of the solar cell performance. To avoid the complete melting of D-sorbitol followed by the crystallization during the cooling which may cause a severe problem for the device, we selected the annealing method in this study.

2.2. Contact Area. In order to compare the contact area of active layer (P3HT:PCBM/PH500(D-sorbitol)) and Ag PET film, we measured the shear strengths of the film hetero-structure by the tensile tester. The higher the adhesion force between the Ag PET film and the active layer, the higher the tensile becomes. Figure 7a,b shows the shear strengths of the cells at different D-sorbitol concentrations and the cells at the fixed contact area but different film thicknesses, respectively. As shown in Figure 7b, the shear strength has less relation to the film thickness. Therefore, it was considered that the shear strength was very closely related to the contact area.[25−29]

From Figure 7a, in the 20 to 40 wt % range, the shear strength remarkably increased. This may be because the contact area was larger. A large contact area may be caused by reducing the glue film shrinkage during cell annealing with an increase in viscosity.

From 40 to 50 wt % of D-sorbitol concentration, a large change in shear strength was not observed despite viscosity change. It was considered that the effect to prevent the film from shrinkage was reduced and the contact area was saturated.

When D-sorbitol concentration was more than 50 wt %, some cracks were observed and reduced the contact area. At 60 wt %, the shear strength was 0.08 N/mm^2, lower than that at 40−50 wt %. At this condition, η_{front} was 0.52 %, lower than that at 40−50 wt %.

2.3. Relationship between Glue Layer's Factors and Photovoltaic Property. To clarify the effects of the film thickness and the contact area on the photovoltaic property, especially, efficiency, we classified two regions: (i) less than 40 wt % and (ii) more than 40 wt % of D-sorbitol concentration in PH500 solution. (i) The predominant factor affecting efficiency is the contact area. The contact area changes with change in viscosity. At these conditions, the photovoltaic property depends on the effect of reducing the interfacial contact resistance between the active layer and Ag film rather than decreasing carrier transport property with an increase in the film thickness. (ii) The decrease in carrier transport property has direct impact on the efficiency. The contact area does not change and may not be the main factor affecting efficiency. Therefore, the film thickness is important for improving the efficiency. This discussion can be explained by the decrease in FF at more than 40 wt %.

These discussions were summarized in Figure 8. In the case of the cells made with less than 40 % of D-sorbitol concentrations, the film shrinkage during annealing was prevented because viscosity dramatically increased. An increase

in viscosity caused an increase in junction area and also improved the interfacial resistance between the glue layer and P3HT:PSBM surface. Therefore, the efficiency was enhanced. However, in the case with more than 40 %, the increase of junction area might be saturated. Instead of this, the increase in film thickness of the glue layer had a great impact on the carrier transport. Therefore, the efficiency decreased. In this work, it is demonstrated that when the film thickness of the glue layer was under 6.6 μm, the energy conversion efficiency depends not on conductivity but on the contact area.

CONCLUSIONS

We fabricated semitransparent polymer-based solar cells by using a lamination process. In our work, it was demonstrated that physical property changes affected the photovoltaic property and investigated the effects on the photovoltaic property by adding D-sorbitol. It was also suggested that the photovoltaic performance depended strongly on the contact area and the film thickness regardless of the conductivity of the conductive glue layer. The optimized devices were semitransparent with power efficiencies of 2.41%. A simple lamination process without using a vacuum process was proposed in this study. This process for semitransparent solar cells will be very effective for the design of bifacial power generating windows.

AUTHOR INFORMATION

Corresponding Author

*E-mail: shiratori@appi.keio.ac.jp.

Notes

The authors declare no competing financial interest.

REFERENCES

(1) Koeppe, R.; Hoeglinger, D.; Troshin, P. A.; Lyubovskaya, R. N.; Razumov, V. F.; Sariciftci, N. S. *ChemSusChem* **2009**, *2*, 309−313.
(2) Lunt, R. R.; Bulovic, V. *Appl. Phys. Lett.* **2011**, *98*, 113305-1−113305-3.
(3) Wilken, S.; Hoffmann, T.; Hauff, E.; Borchert, H.; Parisi, J. *Sol. Energy Mater. Sol. Cells* **2012**, *96*, 141−147.
(4) Winkler, T.; Schmidt, H.; Flügge, H.; Nikolayzik, F.; Baumann, I.; Schmale, S.; Weimann, T.; Hinze, P.; Johannes, H.; Rabe, T.; Hamwi, S.; Riedl, T.; Kowalsky, W. *Org. Electron.* **2011**, *12*, 1612−1618.
(5) Lewis, J.; Lafalce, E.; Toglia, P.; Jiang, X. *Sol. Energy Mater. Sol. Cells* **2011**, *95*, 2816−2822.
(6) Luber, E. J.; Buriak, J. M. *ACS Nano* **2013**, *7* (6), 4708−4714.
(7) Lim, Y. F.; Lee, S.; Herman, D. J.; Lloyd, M. T.; Anthony, J. E.; Malliaras, G. G. *Appl. Phys. Lett.* **2008**, *93*, 193301-1−193301-3.
(8) Peh, R. J.; Lu, Y.; Zhao, F.; Lee., C. L. K.; Kwan, W. L. *Sol. Energy Mater. Sol. Cells* **2011**, *95*, 3579−3584.
(9) Kang, J. W.; Kang, Y. J.; Jung, S.; You, D. S.; Song, M.; Kim, C. S.; Kim, D. G.; Kim, J. K.; Kim, S. H. *Org. Electron.* **2012**, *13*, 2940−2944.
(10) Zhou, Y.; Li, F.; Barrau, S.; Tian, W.; Inganäs, O.; Zhang, F. *Sol. Energy Mater. Sol. Cells* **2009**, *93*, 497−500.
(11) Gaynor, W.; Lee, J. Y.; Peumans, P. *ACS Nano* **2010**, *4*, 30−34.
(12) Zhou, Y.; Cheun, H.; Choi, S.; Potscavage, J. *Appl. Phys. Lett.* **2010**, *97*, 153304-1−153304-3.
(13) Ranby, B. *J. Anal. Appl. Pyrolysis* **1989**, *15*, 237−247.
(14) Eichinger, K.; Kritzinger, F. *Spectrochim. Acta, Part A: Mol. Spectrosc.* **1991**, *47* (5), 661−664.
(15) Zimmermann, B.; Wurfel, U.; Niggemann, M. *Sol. Energy Mater. Sol. Cells* **2009**, *93*, 491−496.
(16) Norman, K.; Madsen, M. V.; Gevorgyan, S. A.; Krebs, F. C. *J. Am. Chem. Soc.* **2010**, *132*, 166883−16892.
(17) Katz, E. A.; Gevorgyan, S.; Orynbayav, M. S.; Krebs, F. C. *Eur. Phys. J. Appl. Phys.* **2007**, *36*, 307−311.
(18) Seemann, A.; Egelhaaf, H. J.; Brabec, C. J.; Hauch, B. A. *Org. Electron.* **2009**, *10*, 1424−1428.
(19) Huang, J.; Li, G.; Yang, Y. *Adv. Mater.* **2008**, *20*, 415−419.
(20) Bailey, B. A.; Reese, M. O.; Olson, D. C.; Shaheen, S. E.; Kopidakis, N. *Org. Electron.* **2011**, *12*, 108−112.
(21) Yuan, Y.; Bi, Y.; Huang, J. *Appl. Phys. Lett.* **2011**, *98*, 063306-1−063306-3.
(22) Peng, B.; Guo, X.; Cui, C.; Zou, Y.; Pan, C.; Li, Y. *Appl. Phys. Lett.* **2011**, *98*, 243308-1−243308-3.
(23) Okada, I.; Shiratori, S. *ACS Appl.Mater. Interfaces* **2013**, *5*, 4144−4149.
(24) Nardes, A. M.; Kemerink, M.; Kok, M. M.; Vinken, E.; Maturova, K.; Janssen, R. A. *Org. Electron.* **2008**, *9*, 727−734.
(25) Nikogeorgos, N.; Hunter, C.A.; Leggett, G.J. *Langmuir* **2012**, *28*, 17709−17717.
(26) Manoharan, M. P.; Haque, M. A. *J. Phys. D: Appl. Phys.* **2009**, *42*, 095304−095310.
(27) Maeno, Y.; Nakayama, Y. *Appl. Phys. Lett.* **2009**, *94*, 012103−012105.
(28) Kanaga Karuppiah, K. S.; Bruck, A. L.; Sundararajan, S. *Tribol. Lett.* **2009**, *36*, 259−267.
(29) Palyacov, B.; Vlassov, S.; Dorogin, L. M.; Kulis, P.; Kink, I.; Lohmus, R. *Surf. Sci.* **2012**, *606*, 1393−1399.